Kinetic Mechanism of Chloramphenicol Acetyltransferase: The Role of Ternary Complex Interconversion in Rate Determination†

Jacqueline Ellis, Clive R. Bagshaw, and William V. Shaw*

Department of Biochemistry, University of Leicester, Leicester, LE1 7RH, U.K.

Received September 6, 1995; Revised Manuscript Received October 24, 1995⊗

ABSTRACT: Chloramphenicol acetyltransferase (CAT) catalyzes the acetyl-CoA-dependent acetylation of chloramphenicol (Cm) by a ternary complex mechanism and with a random order of addition of substrates. A closer examination of the mechanism of the reaction catalyzed by the type III CAT variant (CAT_{III}) has included the measurement of the individual rate constants by stopped-flow fluorimetry at 5 °C. Under all conditions employed, product release from the binary complexes in both forward and reverse reactions was found to be too slow to account for the observed overall rate of turnover for the reaction. Additional, faster routes for product release are achieved via the formation of the *nonproductive* ternary complexes (CAT:3-acetyl-Cm:acetyl-CoA and CAT:CoA:Cm). The release of 3-acetyl-Cm from the binary complex is 5-fold slower than k_{cat} (135 s^{-1} at 5 °C), whereas the dissociation rate constants of 3-acetyl-Cm from the ternary complexes with CoA and acetyl-CoA are 120 and 200 s^{-1}, respectively. Arrhenius plots of dissociation rate constants indicate a slow release of products over a broad temperature range. Computer simulations based on the rate constants of CAT_{III} applied to a ternary complex mechanism, assuming random order of substrate addition and product release, yielded nonlinear initial rates of product formation unless both nonproductive ternary complexes were included in the model. Simulated steady-state kinetic analyses based on the latter assumption yielded kinetic parameters that compared favorably with those determined experimentally. The proton inventory for the reaction catalyzed by CAT_{III} is compatible with the involvement of proton(s) in one or more rate-determining steps, possibly *en route* to the transition state from the ternary complex of enzyme and substrates (Cm and acetyl-CoA). Thus, both product release and ternary complex interconversion are likely to be involved in rate determination of the CAT_{III} reaction.

Chloramphenicol acetyltransferase (CAT)[1] is the most commonly encountered effector of resistance to chloramphenicol (Cm) in eubacteria [reviewed by Shaw and Leslie (1991) and Shaw (1992)]. The inactivation process catalyzed by CAT is reversible, the immediate product of the forward reaction (3-acetyl chloramphenicol, 3-AcCm) being devoid of antibiotic activity by virtue of its low affinity for the peptidyltransferase center of prokaryotic ribosomes (Shaw & Unowsky, 1968). Scheme 1 summarizes the transformations which take place at pH 7.5 when Cm is incubated in the presence of CAT and 2 equiv of acetyl-CoA. The nonenzymic rearrangement of 3-AcCm to form 1-AcCm allows a second round of acetyl transfer from CoA, yielding the 1,3-diacetyl derivative of Cm (1,3-diacetyl-Cm), which, like both monoacetyl products, is not an inhibitor of protein synthesis. The second enzymic acetylation is 40-fold slower than the first step, most probably due to the formation of a sterically unfavorable complex of CAT and 1-acetyl-Cm (Murray et al.,1991).

Scheme 1

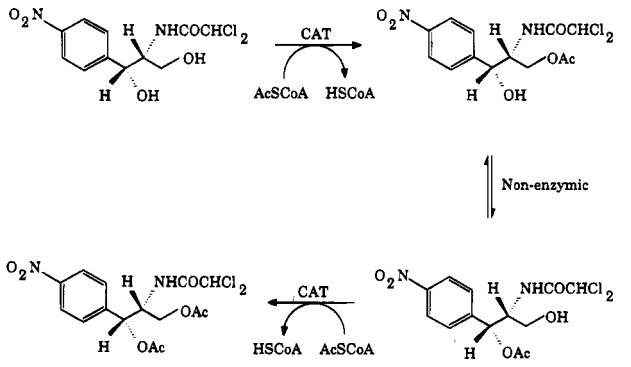

Much is now known of the interaction of CAT and its substrates from (a) crystallographic studies of the binary complexes of enzyme and Cm or CoA at 1.75 and 2.4 Å resolution, respectively (Leslie, 1990; Leslie et al., 1988) and (b) results of spectroscopic experiments (fluorescence, NMR, and IR) with CAT and its ligands in conjunction with structure-based mutagenesis (Ellis et al., 1991; Derrick et al., 1992; Murray et al., 1994). The choice of protein for the above studies, as well as for those described here, has been the type III enzyme (CAT_{III}) which is not only the sole naturally occurring CAT variant to yield diffraction quality crystals but is also the most competent catalytically.

The three equivalent active sites of CAT trimers (3 × 25 kDa) lie at the interfaces between identical subunits; the *S*-acetyl thioester of CoA approaches the catalytic center from one end of a long tunnel (25 Å) traversing the trimer, and the 3-hydroxyl of Cm does so from the opposite direction

† This research was supported by the Science and Engineering Research Council by means of an institutional award supporting a Centre for Research in Molecular Recognition.

* To whom correspondence should be addressed. Tel: +44 116 252 3470. FAX: +44 116 252 3369.

⊗ Abstract published in *Advance ACS Abstracts,* December 1, 1995.

[1] Abbreviations: CAT, chloramphenicol acetyltransferase; CAT_{III}, type III variant of CAT; Cm, chloramphenicol [D-*threo*-1-(4-nitrophenyl)-2-dichloroacetamido-1,3-propanediol]; DTNB, 5,5′-dithiobis(2-nitrobenzoic acid); *p*-cyano-Cm, D-*threo*-1-(4-cyanophenyl)-2-(dichloroacetamido)-1,3-propanediol; TSE buffer, 50 mM Tris/HCl buffer, pH 7.5, containing 100 mM NaCl and 0.1 mM EDTA.

0006-2960/95/0434-16852$09.00/0

Scheme 2

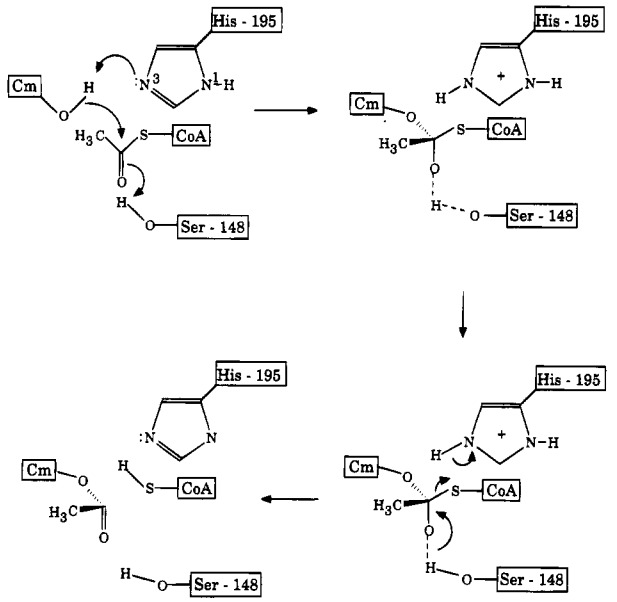

(Leslie et al., 1988). The proposed chemical mechanism (Scheme 2) involves deprotonation of the 3-hydroxyl of the acyl acceptor (Cm) by $N^{\epsilon 2}$ of His-195[2] with attack of the resulting activated oxygen at the thioester carbonyl carbon of acetyl-CoA to yield a tetrahedral intermediate that is stabilized by a shared hydrogen bond with the hydroxyl of Ser-148 (Lewendon et al., 1990).

Data from a steady-state kinetic analysis of the primary acetylation event (and the reverse reaction) were judged to be diagnostic of a sequential mechanism involving the random order of addition of substrates to form a productive ternary complex (Kleanthous & Shaw, 1984). The high value (600 s^{-1}) of the overall rate constant (k_{cat}) and the low (12 μM) dissociation constant (K_m) for Cm in the ternary complex combine to yield a specificity constant (k_{cat}/K_m) of 5.0×10^7 M^{-1} s^{-1} (at 25 °C and pH 7.5), inviting explanations of the efficiency of acetyl transfer to Cm and, in particular, delineation of the rate-determining step for the forward reaction.

Such considerations prompted further studies of the kinetic properties of CAT_{III}, making use of both steady-state and transient methods. The conclusions drawn from the results of the experiments described below are that, whereas the formation of the ternary complex of CAT with both substrates is rapid in both the forward and reverse directions, the rate of product release from the CAT:product binary complexes is low and of the same order as k_{cat}. Kinetic measurements and computer simulations of the reaction course suggest that a minor modification of the proposed mechanism allows catalysis to occur rapidly, unimpeded by slow product release steps, such that interconversion of the central ternary complexes determines the overall rate of the reaction.

EXPERIMENTAL PROCEDURES

Preparation of 3-Acetyl-Cm. 3-Acetyl-Cm was made and purified by the procedure described by Murray et al. (1994).

[2] Alignment of the amino acid sequences of many CAT variants (Shaw & Leslie, 1991) has resulted in a general numbering system which is used here. Ser-148 and His-195 are residues 142 and 189, respectively, in the primary structure of CAT III (Murray et al., 1988).

Preparation of Ethyl-CoA. Ethyl-CoA was prepared from ethyl iodide and CoA as described by Lewendon et al. (1994).

Purification of CAT. CAT_{III} was purified from *Escherichia coli* extracts by affinity chromatography on chloramphenicol–Sepharose resin as described previously (Lewendon et al., 1988). Chloramphenicol used as eluent was removed by gel-permeation chromatography on Sephadex G-50. Enzyme purity was assessed by SDS–polyacrylamide gel electrophoresis, and the concentration of CAT_{III} was determined by its extinction at 280 nm ($\epsilon_{0.1\%} = 1.31$).

Assay of CAT Activity. CAT activity was measured spectrophotometrically at 25 °C in the standard assay mixture containing TSE buffer (pH 7.5), 1 mM 5,5′-dithiobis(2-nitrobenzoic acid), 0.1 mM chloramphenicol, and 0.4 mM acetyl-CoA. The reaction was initiated by the addition of enzyme, and the rate of formation of CoA was monitored by its reaction with DTNB and liberation of the thionitrobenzoate dianion ($\epsilon_{412nm} = 13\,600$ M^{-1} cm^{-1}). One unit of enzyme activity is defined as the amount of enzyme converting 1 μmol of substrate to product per minute under the standard assay conditions.

For the steady-state kinetic analysis of the forward transacetylation reaction and substrate inhibition experiments, the concentrations of chloramphenicol and acetyl-CoA were varied in the standard assay mixture. Kinetic parameters were determined as described previously (Kleanthous & Shaw, 1984). Steady-state kinetic assays of the reverse transacetylation reaction were performed by coupling the production of acetyl-CoA to the reduction of NADH by using malate dehydrogenase and citrate synthase (Kleanthous & Shaw, 1984).

Proton Inventory. The steady-state kinetic analysis was performed as above but at various mole fractions of deuterium in the solvent to produce a proton inventory (Schowen, 1977). The relative k_{cat} data were plotted as a function of the mole fraction of deuterium in the mixed isotopic solvent and fitted to the Kresge formulation of the Gross–Butler equation (eq 1) by nonlinear regression using the computer program Grafit (Erithacus Software, 1993) assuming, first, one-proton catalysis and, second, multiproton catalysis

$$k_n/k_H = (1 - n + n\phi^T)^P \quad (1)$$

where n is the fraction of deuterium in the mixed isotopic solvent, ϕ^T is the deuterium fractionation factor of the transition state, k_H is the rate in H_2O, k_n is the rate at n, and P is the number of protons contributing to the isotope effect.

Stopped-Flow Fluorimetry. A SF-17MV stopped-flow spectrometer (Applied Photophysics, Leatherhead, U.K.) was used for the measurement of association and dissociation rate constants as described by Ellis et al. (1991b). The dead time of the instrument was determined to be 1.6 ms from the kinetics of formation of the fluorescent magnesium 8-hydroxyquinoline chelate complex (Brissette et al., 1989).

Computer Simulations. The computer program KSIM (Neil C. Millar, personal communication) was used to simulate the time course of the enzymic reaction according to the rates measured by stopped-flow fluorimetry input into the defined kinetic model. The rate equations generated were solved by the Runge–Kutta algorithm, and the solutions were

Table 1: Steady-State Kinetic Parameters for Chloramphenicol Acetyltransferase[a]

Forward Reaction: Acetylation of Chloramphenicol					
		chloramphenicol		acetyl-CoA	
temp (°C)	k_{cat}	K_d	K_m	K_d	K_m
25	599	4.0	12.0	31.0	90.0
5	135	2.6	8.8	28.8	96.1
Reverse Reaction: Acetylation of CoA					
		3-acetyl-chloramphenicol		CoA	
temp (°C)	k_{cat}	K_d	K_m	K_d	K_m
25	71	23.0	48.9	40.7	86.5
5	12	4.9	11.7	24.7	59.2

[a] Since the mechanism involves a random order of addition of substrates to form the productive ternary complex, the K_d values are dissociation constants for binary complexes whereas K_m refers to the same parameter for ternary complexes. All k_{cat} values are in s^{-1}, and all K_d and K_m values are in μM.

presented graphically as the time course of reaction intermediate concentrations.

RESULTS

Steady-State Kinetic Parameters. The forward and reverse transacetylation reactions catalyzed by CAT were characterized at 5 °C by steady-state kinetic analysis. The kinetic parameters obtained are compared in Table 1 with those described previously for the forward reaction at 25 °C and more recently in our laboratory by A. Lewendon for the reverse reaction (unpublished results). Since k_{cat} (~600 s^{-1}) must be the lowest and, therefore, limiting value at 25 °C for steps on the forward reaction pathway, it seemed certain that the characterization of individual steps at that temperature would be beyond the capabilities of available stopped-flow methodology. The 4.5-fold reduction in k_{cat} observed at 5 °C made it likely that the collection of reliable and relevant transient kinetic data by stopped-flow techniques would be feasible at the lower temperature.

To explore the possibility that a change in the rate-limiting step might occur between the two temperatures, the study was extended to determine steady-state kinetic parameters at a number of temperatures from 5 to 30 °C. The Arrhenius plot constructed from k_{cat} determinations over this, albeit limited, temperature range was observed to be linear, indicating either that no change in the rate-limiting step was involved or that all steps which were limiting had similar activation energies (Figure 1a). The heat of activation (ΔH) for the reaction, calculated from the slope of the plot, was estimated to be +11.3 kcal mol^{-1}.

Substrate Inhibition. Initial rates for the CAT reaction were measured over a range of substrate concentrations, from $0.5K_m$ to $50K_m$, in an extension of the steady-state kinetic analysis described above. Although the absence of substrate inhibition (see Figure 2) in a random-order ternary complex mechanism is normally taken as evidence for a rapid equilibrium mechanism (Cornish-Bowden, 1979), the situation with respect to CAT_{III} is more complicated (see Discussion).

Proton Inventory. A proton inventory constructed for the forward transacetylation reaction showed an intense dependence of k_{cat} on the concentration of deuterium in the solvent. When plotted as a ratio of k_{cat} (n% D_2O) to k_{cat} in 100%

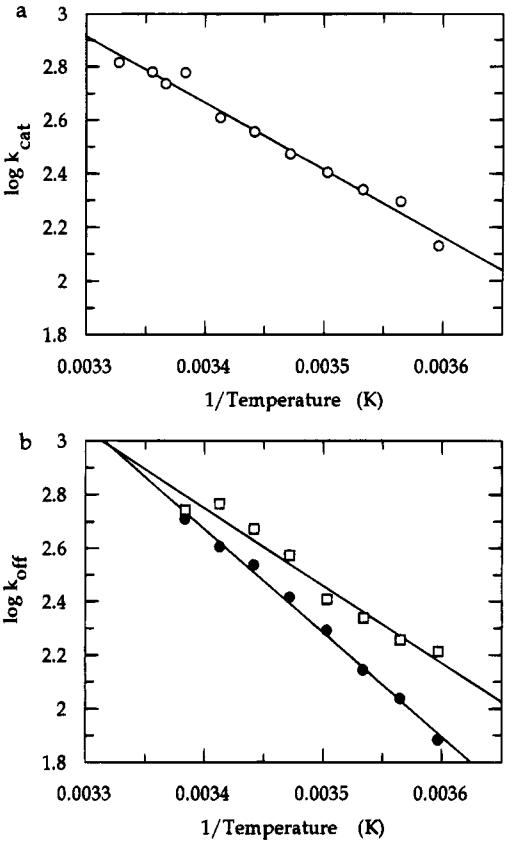

FIGURE 1: Arrhenius plots of (a) k_{cat} from steady-state kinetic analysis data and (b) dissociation rate constants of 3-acetyl-Cm (●) and CoA (□) from the respective binary complex with CAT_{III} measured at a range of temperatures.

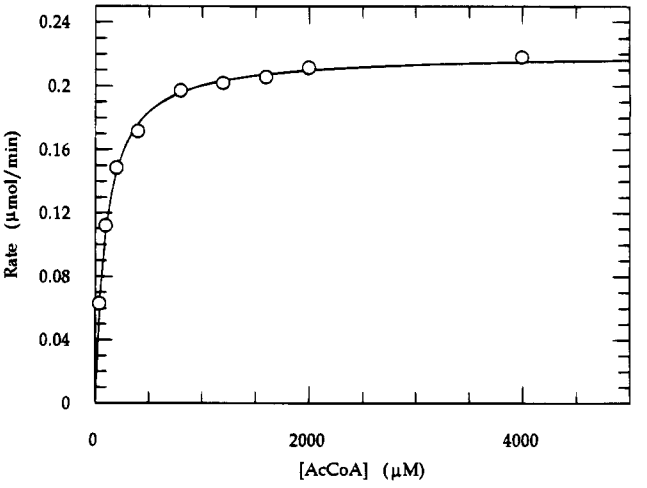

FIGURE 2: The effect of acetyl-CoA concentration on the steady-state reaction rate. The concentration of chloramphenicol was maintained at 100 μM. Analysis of the data by nonlinear regression to a hyperbola yields a binding constant of 98 μM.

H_2O against the mole fraction of deuterium, the data describe an apparent exponential relationship in which $n = 12$ when fitted to eq 1, emphasized by the random distribution in the residuals plot (Figure 3). Although such an observation is consistent with multiproton catalysis (generalized solvent isotope effect) (Schowen, 1977), it should be noted that simple linear regression also gives an acceptable fit if no special weighting is given to the first point (no D_2O) of Figure 3. However, it is useful to recall that the Gross–Butler equation was formulated on the premise that a single

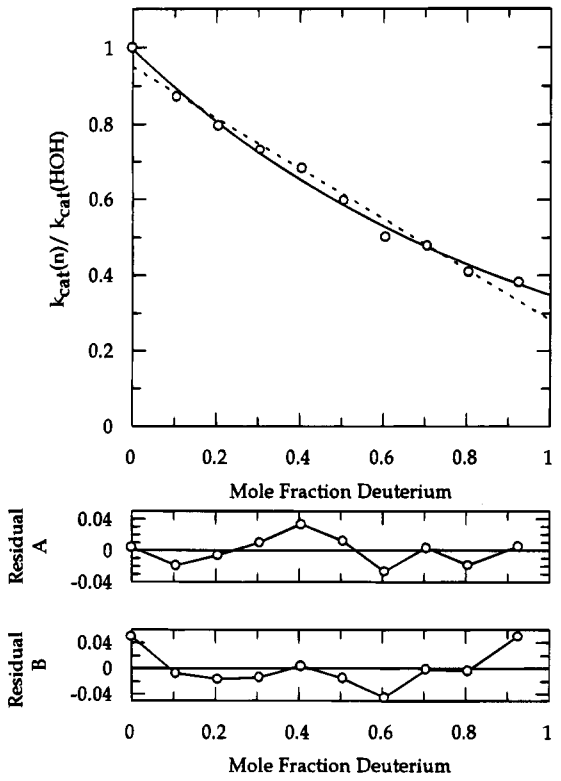

FIGURE 3: Proton inventory constructed from steady-state kinetic analysis data measured over a range of deuterium content in the solvent to show the variation of k_{cat} with mole fraction of deuterium. The solid line shows an exponential curve fitted to the data according to eq 1 where $n = 12$ (residual errors shown in plot A). A linear fit (- - -) is also illustrated along with the residual error (residual plot B).

step determines the reaction rate, an assumption that is less than certain for CAT_{III} (Kiick, 1991). Hence, the form of the proton inventory curve is less important than the magnitude of the isotope effect, which by itself implies that proton transfer must be involved in one or more steps contributing to rate limitation.

Transient Kinetics. Binary Complex Formation and Substrate Dissociation: Cm Binding. Chloramphenicol binding to CAT_{III} produces a substantial quench in protein fluorescence (−29%; Ellis et al., 1991a). At 25 °C the association rate can only be observed over a narrow range of Cm concentrations (typically from $0.5K_d$ to $2K_d$) before the rate exceeds instrumental limits, yielding an association rate constant of 4.8×10^7 M^{-1} s^{-1} from a plot of k_{obs} as a function of [S]. Back-extrapolation of the data to zero [Cm] yields a dissociation rate constant of ~200 s^{-1} (Ellis et al., 1991b). At lower temperatures (5 °C), it is possible to use a wider range of [Cm] while still satisfying the requirement [E] ≪ [S] for a pseudo-first-order reaction, producing reliable values for k_{on} (8.9×10^6 M^{-1} s^{-1}) and k_{off} (34 s^{-1}).

The dissociation rate constant for Cm can also be determined independently. Unlike Cm itself, the *p*-cyano analogue of the antibiotic produces no change in protein fluorescence and hence may be used in the Cm displacement assay described previously (Ellis et al., 1991b). The latter method yielded $k_{off} = 26$ s^{-1} at 5 °C and 207 s^{-1} at 25 °C, both of which compare favorably with those described above.

The K_d values for Cm derived from the above kinetic data (k_{off}/k_{on}) are 2.9 and 4.1 μM at 5 and 25 °C, respectively. Both values compare favorably with those derived independently from equilibrium methods (Ellis et al., 1991b).

Acetyl-CoA Binding. Under equilibrium conditions at 25 °C the binding of acetyl-CoA to CAT_{III} results in a 25% enhancement of intrinsic protein fluorescence (Ellis et al., 1991a). Despite this, the association of acetyl-CoA with CAT_{III} yielded biphasic traces wherein a maximum total amplitude change of ~9% was observed in the stopped-flow apparatus at 5 °C. The maximum observed rate constants were 190 and 20 s^{-1} for the two-component phases, respectively, each of which was attained via a hyperbolic dependence on the concentration of acetyl-CoA. It is difficult to partition the component amplitudes of a biphasic process accurately. However, the total increase in fluorescence observed remained constant (9%) over the entire range of acetyl-CoA concentrations employed (10−400 μM).

The dissociation rate constant of acetyl-CoA was estimated to be 81 s^{-1} by the displacement of acetyl-CoA by CoA. When taken together with the independently determined K_d for acetyl-CoA (28.8 μM), an association rate constant of 2.8×10^6 M^{-1} s^{-1} can be calculated.

The results suggest that the binding of acetyl-CoA to free CAT_{III} may be at least a two-step process, with an unseen and probably very fast phase (accounting for the missing amplitude) and a much slower phase that can be observed but is too slow to be on the actual catalytic pathway.

Ethyl-CoA Binding. Ethyl-CoA, a non-hydrolyzable thioether analogue of acetyl-CoA, was included in this study for the convenience of being able to produce a stable (nonproductive) ternary complex. Unlike the biphasic traces seen for acetyl-CoA, the association of ethyl-CoA with CAT_{III} produced an exponential increase in fluorescence intensity, but once again, the rate constant showed a hyperbolic dependence on concentration, suggesting a multistep binding process. As observed for acetyl-CoA, the amplitude change remained constant across the concentration range used. The maximum rate constant observed was 180 s^{-1}. The dissociation rate constant from the binary complex, obtained by displacement of ethyl-CoA by CoA, was found to be 107 s^{-1} at 5 °C.

Formation/Dissociation of Ternary Complexes: Cm Binding to CAT:Ethyl-CoA Complex. Since the fluorescence responses arising from the formation of the two different binary complexes of enzyme and substrate in the forward reaction involve a quench on the one hand (Cm) and an enhancement on the other (acetyl-CoA), it follows that the formation of the ternary complex is bound to be associated with a complex fluorescence signal. Hence, the binding of Cm to the CAT:acetyl-CoA binary complex was not investigated, inasmuch as any associated fluorescence changes could originate from several different species due to the equilibria between binary and ternary complexes of both substrates and products. Although it is an imperfect (noncarbonyl) analogue of acetyl-CoA, ethyl-CoA forms a nonproductive ternary complex with CAT_{III} and Cm and hence offered the prospect that measurements could be interpreted with more confidence, albeit with qualifications.

In the presence of ethyl-CoA at 400 μM ($K_i = 103$ μM in the ternary complex at 25 °C; P. J. Day, unpublished results), the association rate constant for Cm at 5 °C was essentially the same as for the binary complex whereas the dissociation rate constant increased from 26 to 112 s^{-1} (Table 2). Such a 4-fold increase in the Cm dissociation rate constant accounts for the known lower affinity of the substrate in the ternary complex (K_m) as compared with the CAT:Cm binary

Table 2: Kinetic Parameters at 5 °C for the Binary and Ternary Complexes of Chloramphenicol Acetyltransferase and Its Substrates (or Products)

step no.[a]	ligand[b]	association rate constant[c] (μM^{-1} s^{-1})	dissociation rate constant (s^{-1})
1	Cm	10	26
2	acetyl-CoA	2.8	81
3	acetyl-CoA	5.7	560[d]
4	Cm	12.7	112[d]
5	interconversion	nd[e]	nd
6	CoA	5.0	300
7	3-acetyl-Cm	10.0	120
8	3-acetyl-Cm	5.1	25
9	CoA	6.5	160
10	acetyl-CoA	8.2	400
11	3-acetyl-Cm	7.0	200
12	Cm	10.7	26
13	CoA	5.0	400

[a] The step number refers to the kinetic steps defined in Scheme 4. [b] The named ligand is the associating/dissociating ligand of the step. [c] Calculated from equilibrium binding constants. [d] Ethyl-CoA used in place of Acetyl-CoA. [e] Not determined.

complex (K_d). In contrast, the presence of CoA had no effect on Cm binding or release.

Acetyl-CoA Binding to CAT:p-Cyano-Cm Complex. By using the *p*-cyano analogue of Cm, it was possible to characterize the binding of acetyl-CoA to form a ternary complex under defined conditions; namely, saturating *p*-cyano-Cm (at 100 μM; $\sim 10K_m$) to ensure that the ternary complex was the dominant species present. When free enzyme from one syringe was mixed with *p*-cyano-Cm and acetyl-CoA from the second syringe, the binding of acetyl-CoA was observed as an exponential increase in fluorescence intensity, the rate constant of which varied hyperbolically with [acetyl-CoA] to reach a maximum rate of ~ 180 s^{-1}. The slower phase seen on binding to form the CAT:acetyl-CoA binary complex was not observed on forming the ternary complex. When the enzyme was preincubated with *p*-cyano-Cm, there was no detectable fluorescence change seen on binding acetyl-CoA, the conclusion being that the slow step(s) involved in acetyl-CoA binding had been abolished.

The dissociation rate constant for ethyl-CoA from the ternary complex with Cm was ~ 560 s^{-1} at 5 °C, measured by displacement with CoA. The observed rate constant is 5-fold greater than that measured for the ethyl-CoA:CAT binary complex and, as observed similarly with Cm, accounts for the decrease in affinity observed previously of CAT_{III} for acetyl-CoA seen on proceeding from binary to ternary complex (Ellis et al., 1991b). The relatively large dissociation rate constant implies that the slower rate (180 s^{-1}) observed in the association reactions above is not an integral part of the kinetic mechanism but probably reflects a perturbation of bound acetyl-CoA within its binding pocket in the binary complex, a state not detected when the second substrate is already bound.

Product Release: CoA. CoA release from the ternary complex of products with CAT_{III} was examined. Although the amplitude is small (2.7%), the dissociation rate constant was found to be approximately 300 s^{-1} at 5 °C by displacement with acetyl-CoA.

CoA dissociates from the binary complex with CAT_{III} at a rate constant of about 160 s^{-1}, which is similar to the value of k_{cat} (135 s^{-1}). Therefore the experiment was measured

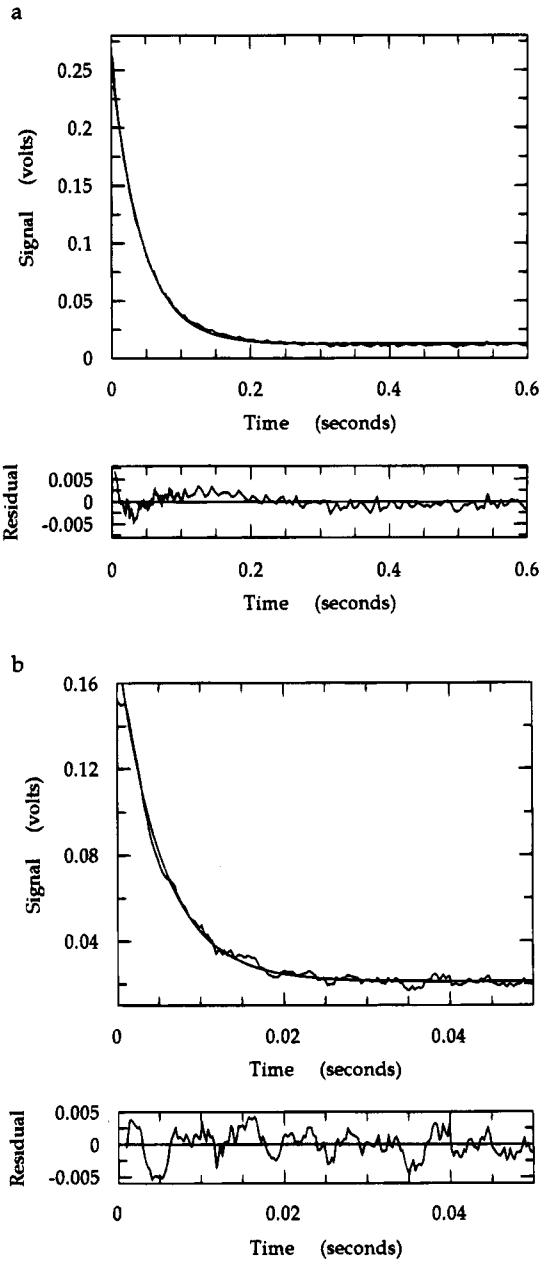

FIGURE 4: Stopped-flow records of the dissociation of 3-acetyl-Cm from (a) binary and (b) ternary complex at 5 °C. (a) Dissociation of 3-acetyl-Cm from protein alone. One syringe contained 100 μM *p*-cyano-Cm, and the other contained 50 μM 3-acetyl-Cm and 5 μM CAT. An exponential fit is superimposed on the decay phase and yields a rate constant of 24 s^{-1}. The data shows a 22% enhancement of protein fluorescence. (b) Dissociation of 3-acetyl-Cm from the ternary complex with protein and acetyl-CoA. One syringe contained 400 μM acetyl-CoA and 100 μM *p*-cyano-Cm, and the other contained 400 μM acetyl-CoA, 50 μM 3-acetyl-Cm, and 5 μM CAT. The superimposed exponential fit yields a rate constant of 202 s^{-1}. The data shows a 15% enhancement of fluorescence. A residual plot is shown below each graph.

over a number of temperatures until it was too fast to measure. On plotting $\log(k_{off})$ against $1/T$, a linear fit extrapolates to a rate constant of ~ 750 s^{-1} at 25 °C (Figure 1b).

Interestingly, the presence of Cm in a ternary complex with CoA and CAT_{III} (another complex not on the reaction pathway) accelerates the release of CoA to >400 s^{-1} at 5 °C.

3-Acetyl-Cm. 3-Acetyl-Cm is released from the ternary complex (CAT:CoA:3-acetyl-Cm) with a rate constant of

Scheme 3

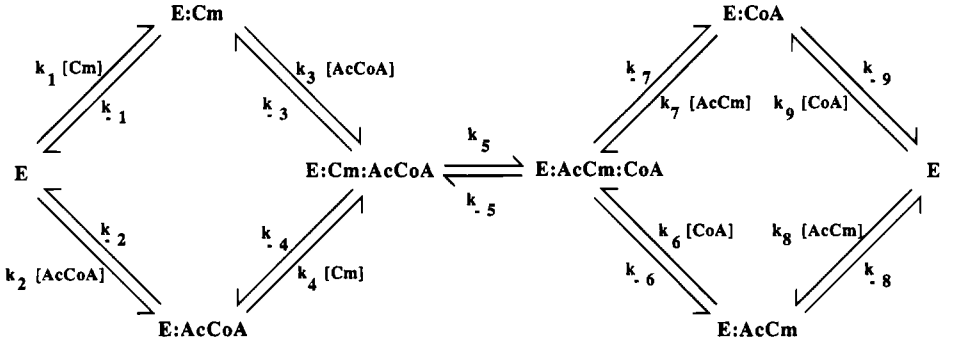

~120 s^{-1} at 5 °C. Traces were typically biphasic, and a second, slower rate constant (25 s^{-1}) accounted for two-thirds of the total amplitude (−22%). The second phase can be safely attributed to the release of Cm, formed from the reverse reaction, with some contribution from binary complex release of 3-acetyl-Cm. Release of 3-acetyl-Cm from a ternary complex with acetyl-CoA, a complex not on the kinetic pathway, is around 200 s^{-1} (Figure 4b).

Nonetheless, the measured rate constant for release of 3-acetyl-Cm from the binary complex (CAT:3-acetyl-Cm) is only 25 s^{-1}, which is too slow for the forward reaction at 5 °C (Figure 4a). The rate of release of 3-acetyl-Cm from the binary complex was measured over a range of temperatures, and an Arrhenius plot was constructed (Figure 1b). The linearity of the plot yields the conclusion that 3-acetyl-Cm is released at a similarly "slow rate" at 25 °C (~500 s^{-1} compared to $k_{cat} \approx 600$ s^{-1}). The implication of this inference is that 3-acetyl-Cm is the first product to leave or needs to be displaced by the incoming acetyl-CoA.

Computer Simulation of Kinetic Data. Kinetic data were generated by the computer program KSIM to determine the consequences of kinetic model and ternary complex interconversion rates on the steady-state kinetic parameters. The concentrations of enzyme and substrates used in simulations were the same as those chosen for steady-state kinetic analysis and substrate inhibition experiments. The rate of the appearance of free product (CoA) in each simulation was treated and plotted as real data to yield steady-state kinetic parameters.

The first model used was that depicted in Scheme 3. The rate constants for each individual step at 5 °C were those described in Table 2, and the rate constant for ternary complex interconversion (k_5) was set first at 135 s^{-1} and then at 1000 s^{-1} while maintaining k_{-5} at 50 s^{-1}. (Thermodynamic balance was maintained by slight adjustments of the second-order rate constants.) In each simulation, the appearance of free product showed a nonlinear increase in concentration due to product inhibition via the accumulation of binary complexes (Figure 5).

The second model used was that represented by Scheme 4. Under the same conditions described above, the appearance of free product was linear over the entire 60 s of each simulation and much faster than in Scheme 3 (Figure 5). The rapid attainment of the steady state allowed the calculation of "simulated" kinetic parameters for each input interconversion rate (Table 3). There was no evidence of substrate inhibition when the concentration of either substrate was set as $50K_m$.

Finally, each model was used to simulate the reverse reaction catalyzed by CAT_{III}. In this case, k_{-5} was chosen

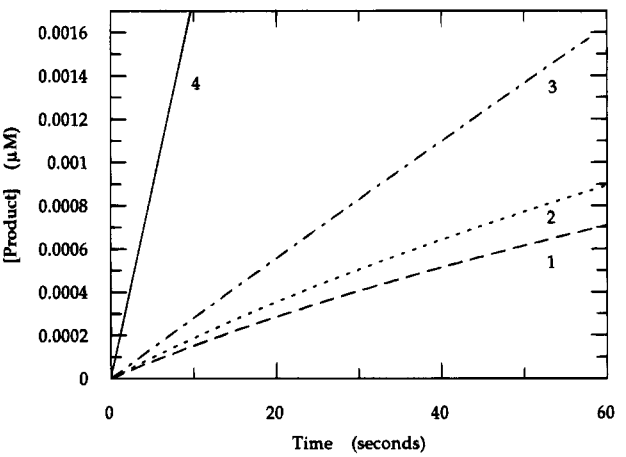

FIGURE 5: The generation of free product with time as predicted by simulations based on Schemes 3 and 4 with individual rate constants as defined in Table 2. Substrate concentrations were set to 20 μM Cm and 200 μM acetyl-CoA, whereas the total enzyme concentration was 0.5 nM with k_{-5} set to 50 s^{-1}. Curves 1 and 2 are the results of simulations based on Scheme 3 in which k_5 is defined as 135 and 1000 s^{-1}, respectively. Curves 3 and 4 are the results of simulations based on Scheme 4 in which k_5 is defined to be 135 and 1000 s^{-1}, respectively.

to be 12, 50, and 100 s^{-1}, while maintaining $k_5 = 1000$ s^{-1} and maintaining thermodynamic balance by adjusting the second-order rate constants. As observed for the forward reaction, the first model (Scheme 3) yielded a nonlinear increase in the concentration of free product. However, the model based on the mechanism shown in Scheme 4 yielded linear increases in free product concentration and allowed the calculation of those kinetic parameters for the reverse reaction included in Table 3.

DISCUSSION

CAT_{III} has been reported to act by a rapid equilibrium random-order ternary complex mechanism (Scheme 3; Kleanthous & Shaw, 1984). There is no evidence to refute the proposition that the substrates may bind in any order in both the forward and reverse reactions. Similarly, the linearity of the reciprocal kinetic plots appears to support the rapid equilibrium assumption, as does the lack of substrate inhibition reported here. Nonetheless, the rapid equilibrium assumption requires not only that interconversion of ternary complexes be rate-limiting and that all other steps are in rapid equilibrium but also implies that rates of product release are significantly greater than the rates of interconversion for the central (ternary) complexes. However, the fact that at 5 °C, where $k_{cat} = 135$ s^{-1}, CoA and 3-acetyl-Cm dissociate at rates of ~160 s^{-1} and ~25 s^{-1} from their

Scheme 4

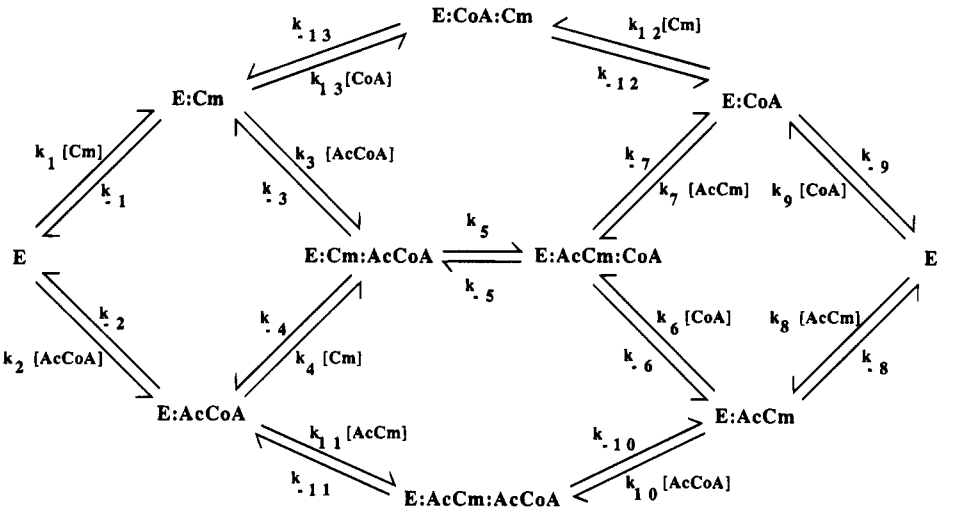

Table 3: Steady-State Kinetic Parameters for the CAT_{III} Reaction Derived from Simulations[a]

Forward Reaction: Acetylation of Chloramphenicol

		chloramphenicol		acetyl-CoA	
k_5	k_{cat}	K_d	K_m	K_d	K_m
135	69	1.8	11.2	10.3	63.1
1000	127	1.8	12.7	5.3	38.6

Reverse Reaction: Acetylation of CoA

		3-acetyl-chloramphenicol		CoA	
k_{-5}	k_{cat}	K_d	K_m	K_d	K_m
12	6.8	4.8	11.3	25.1	59.1
50	12.4	5.3	10.2	22.3	42.8
100	19.6	5.6	9.3	19.8	32.8

[a] All k_5, k_{-5}, and k_{cat} values are in s^{-1}, and all K_d and K_m values are in μM.

respective binary complexes with CAT contradicts the rapid equilibrium assumption and demands an alternative mechanism for product release to override a step that is slower than k_{cat}. Computer simulations based on Scheme 3 imply that such a mechanism would neither be fast enough nor give linear initial rates (Figure 5). Since the Arrhenius plot for k_{cat} (Figure 1a) is linear between 5 and 25 °C; the same situation must prevail at the standard temperature (25 °C). Indeed, the Arrhenius plots for product release support this slow release of products over the entire experimental range of temperatures. In addition, product release in the reverse reaction is also too slow, when compared to turnover rate, to be in keeping with a rapid equilibrium mechanism.

The conclusions to be drawn from the linear Arrhenius plot for k_{cat} are necessarily limited. Although the data are consistent with there being a single rate-determining step for CAT_{III}, the range of temperatures examined (35 K) is not very great, and it should be recognized that rate contributions from steps with similar activation enthalpies would also yield a linear Arrhenius plot. Hence, the experimental data are supportive rather than conclusive.

A model involving random order of addition of substrates followed by compulsory order of product release is unlikely as the reverse reaction also shows random-order binding of substrates. Were the release of a single product from its binary complex to be rate limiting, a close similarity of the gradients of the Arrhenius plots for k_{cat} and for loss of that product would be expected. In fact, the slope in the former case is -2.3 kcal mol^{-1} whereas those for CoA release and 3-acetyl-Cm release are -2.9 and -3.9 kcal mol^{-1} respectively.

Two observations suggest a mechanism by which slow release of products from their binary complexes may be accommodated in an overall fast reaction: acetyl-CoA displaces 3-acetyl-Cm (k_{-11}) at a rate ($\sim$200 s^{-1}) somewhat faster than k_{cat}, and the presence of Cm accelerates the release of CoA (k_{-13} = $\sim$400 s^{-1}). Scheme 4 actually represents the complete ternary complex mechanism for a two-substrate, two-product reaction, assuming that the substrates bind to and products are released from the enzyme in a random order. Nonproductive complexes such as CAT:Cm:CoA and CAT:AcCoA:AcCm are normally assumed to be kinetically significant only at high concentrations of substrates (Cm and CoA or acetyl-CoA and 3-acetyl-Cm) and hence are at risk of being ignored in simple treatments. Nonetheless, it has been demonstrated that acetyl-CoA and 3-acetyl-Cm can bind to CAT_{III} to form a ternary complex, as can Cm and CoA (Ellis et al., 1991b). By including such steps in a simulation of the reaction scheme, it is possible to produce overall rates that are comparable to observed k_{cat} values and to achieve linear initial rates. Furthermore, by performing a series of simulated reactions at varying substrate concentrations, a predictive kinetic analysis of Scheme 4 yields "steady-state kinetic parameters" similar to those observed in the laboratory (Table 3). Despite the complexity of the proposed scheme, it is the rate of interconversion of the central ternary complexes that affects the overall reaction rate (k_{cat}) most profoundly. Such an outcome supports a mechanism for CAT_{III}, wherein product release from the binary and nonproductive ternary complexes is slow but, due to the multiple routes available for release, can only be rate determining if the rates for the reversible interconversion of the central complexes are substantially greater than $\sim$1000 s^{-1} (k_5) and 50 s^{-1} (k_{-5}) in the forward and reverse reactions, respectively.

The chemical steps involved in the conversion of the substrate ternary complex to the product ternary complex for the forward reaction that are reflected in k_5 include (a) deprotonation of the 3-hydroxyl of Cm, (b) attack of the resulting oxyanion at the carbonyl carbon of the thioester of acetyl-CoA, and (c) collapse of the tetrahedral transition-

state intermediate to yield bound products (Scheme 2). Circumstantial evidence suggests that the formation and stabilization of the transition state are probably a concerted process that is dominated by the chemical steps involving proton transfer and the involvement of a critical hydrogen bond. Indeed, the proton inventory data (Figure 3) demonstrate a substantial solvent isotope effect with a dependence on the mole fraction of D_2O that is compatible with the involvement of proton(s) in at least one of the steps contributing to rate limitation (Scheme 2). That a single proton "in flight" must be an oversimplification is suggested in Scheme 2, which also emphasizes the importance of the proton of the hydroxyl of Ser-148, a conserved residue that has been shown to be involved in transition-state stabilization (Lewendon et al., 1990). Since the rates of product release from the S148A variant of CAT_{III} are similar to those for the wild type enzyme (data not shown) it is clear that the 50-fold reduction in k_{cat} due to the loss of the hydroxyl of Ser-148 must reflect a loss of transition-state stabilization in the interconversion of the substrate and product ternary complexes. Taken together with the results of the transient kinetic experiments reported here and the implications of the simulations discussed above, the solvent isotope effect and the results with Ala-148 CAT suggest that an important contribution to rate determination for the reaction catalyzed by CAT_{III} must arise *en route* to transition-state stabilization from the substrate ternary complex.

ACKNOWLEDGMENT

We thank Dr. Ann Lewendon for the results of a steady-state kinetic study of the reverse transacetylation reaction reaction at 25 °C and Dr. Neil C. Millar for the use of his simulation program, KSIM. We are grateful to one of the referees for helpful comments.

REFERENCES

Brissette, P., Ballou, D. P., & Massey, V. (1989) *Anal. Biochem. 181,* 234.
Cornish-Bowden, A. (1979) *Fundamentals of Enzyme Kinetics,* 1st ed., pp 99−129, Butterworth & Co. (Publishers) Ltd., London.
Derrick, J. P., Lian, L.-Y., Roberts, G. C. K., & Shaw, W. V. (1992) *Biochemistry 31,* 8191.
Ellis, J., Murray, I. A., & Shaw, W. V. (1991a) *Biochemistry 30,* 10799.
Ellis, J., Bagshaw, C. R., & Shaw, W. V. (1991b) *Biochemistry 30,* 10806.
Kiick, D. M. (1991) *J. Am. Chem. Soc. 113,* 8499.
Kleanthous, C., & Shaw, W. V. (1984) *Biochem. J. 251,* 211.
Leslie, A. G. W. (1990) *J. Mol. Biol. 213,* 167.
Leslie, A. G. W., Moody, P. C. E., & Shaw, W. V. (1988) *Proc. Natl. Acad. Sci. U.S.A. 85,* 4133.
Lewendon, A., Murray, I. A., Kleanthous, C., Cullis, P. M., & Shaw, W. V. (1988) *Biochemistry 27,* 7385.
Lewendon, A., Murray, I. A., Shaw, W. V., Gibbs, M. R., & Leslie, A. G. W. (1990) *Biochemistry 29,* 2075.
Lewendon, A., Murray, I. A., Shaw, W. V., Gibbs, M. R., & Leslie, A. G. W. (1994) *Biochemistry 33,* 1944.
Murray, I. A., Hawkins, A. R., Keyte, J. W., & Shaw, W. V. (1988) *Biochem J. 252,* 173.
Murray, I. A., Lewendon, A., Williams, J. A., Cullis, P. M., & Shaw, W. V. (1991) *Biochemistry 30,* 3763.
Murray, I. A., Derrick, J. P., White, A. J., Drabble, K., Wharton, C. W., & Shaw, W. V. (1994) *Biochemistry 33,* 9826.
Schowen, R. L. (1977) in *Isotope Effects on Enzyme-Catalyzed Reactions* (Cleland, W. W., O'Leary, M. H., & Northrop, D. B., Eds.) pp 64−99, University Park Press, Baltimore, MD.
Shaw, W. V. (1992) *Sci. Prog. (Oxford) 76,* 565.
Shaw, W. V., & Unowsky, J. (1968) *J. Bacteriol. 95,* 1976.
Shaw, W. V., & Leslie, A. G. W. (1991) *Annu. Rev. Biophys. Biophys. Chem. 20,* 363.

BI9521203